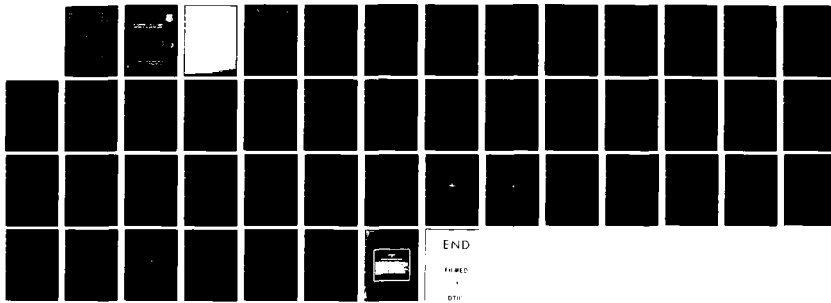
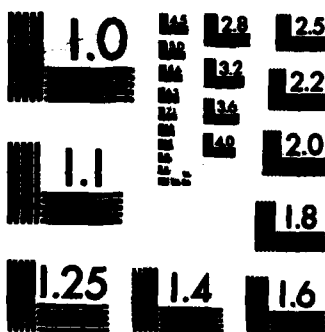
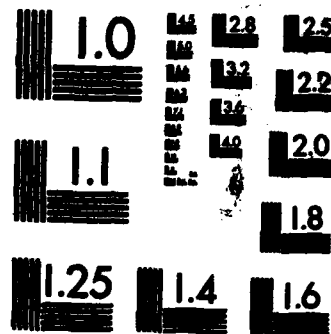


RD-A120 486 AN ALGORITHM TO SELECT ELEMENT LOCATIONS OF AN ADAPTIVE 1/1
ARRAY(U) OHIO STATE UNIV COLUMBUS ELECTROSCIENCE LAB
I J GUPTA ET AL JUN 82 ESL-711679-7 RADC-TR-82-184
UNCLASSIFIED F38602-79-C-0068 F/G 20/14 NL

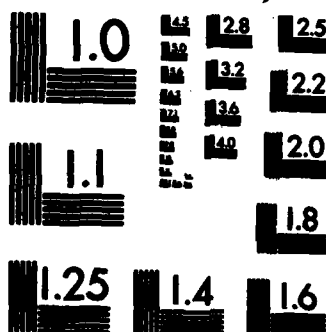




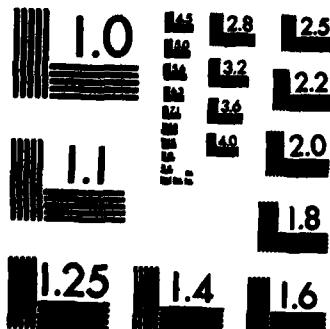
MICROCOPY RESOLUTION TEST CHART
NATIONAL BUREAU OF STANDARDS-1963-A



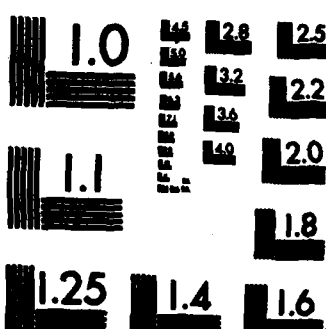
MICROCOPY RESOLUTION TEST CHART
NATIONAL BUREAU OF STANDARDS-1963-A



MICROCOPY RESOLUTION TEST CHART
NATIONAL BUREAU OF STANDARDS-1963-A



MICROCOPY RESOLUTION TEST CHART
NATIONAL BUREAU OF STANDARDS-1963-A



MICROCOPY RESOLUTION TEST CHART
NATIONAL BUREAU OF STANDARDS-1963-A

AD A120486

RADC-TR-82-184
Interim Report
June 1982



AN ALGORITHM TO SELECT ELEMENT LOCATIONS OF AN ADAPTIVE ARRAY

The Ohio State University ElectroScience Lab

Inder J. Gupta and W. D. Burnside

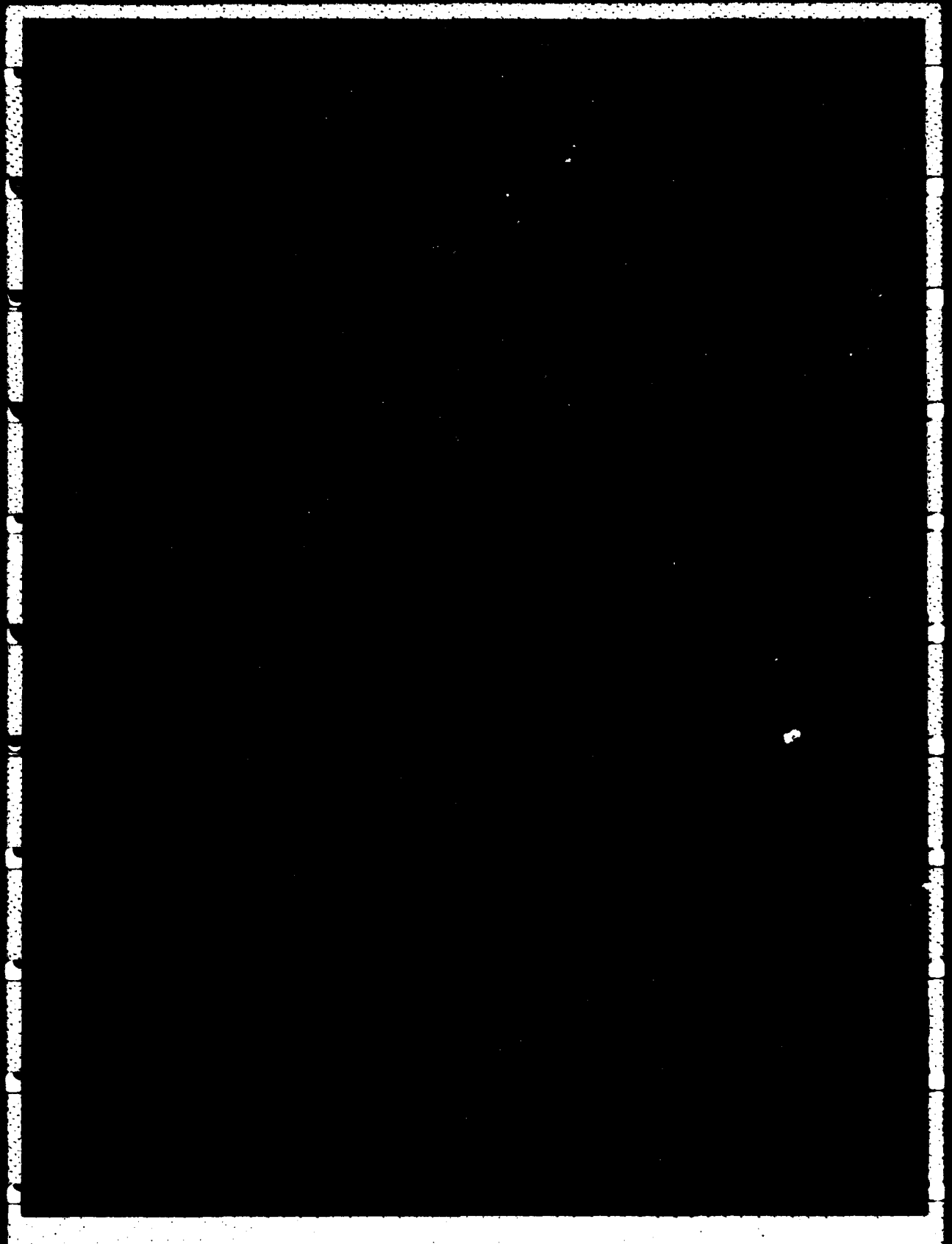
102
S DTIC
ELECTED
OCT 19 1982
D
F

APPROVED FOR PUBLIC RELEASE; DISTRIBUTION UNLIMITED

DTIC FILE COPY

**ROME AIR DEVELOPMENT CENTER
Air Force Systems Command
Griffiss Air Force Base, NY 13441**

82 10 19 012



UNCLASSIFIED

SECURITY CLASSIFICATION OF THIS PAGE (When Data Entered)

REPORT DOCUMENTATION PAGE		READ INSTRUCTIONS BEFORE COMPLETING FORM
1. REPORT NUMBER RADC-TR-82-184	2. GOVT ACCESSION NO. AD-A120486	3. RECIPIENT'S CATALOG NUMBER
4. TITLE (and Subtitle) AN ALGORITHM TO SELECT ELEMENT LOCATIONS OF AN ADAPTIVE ARRAY		5. TYPE OF REPORT & PERIOD COVERED Interim Report September 80 - September 81
7. AUTHOR(s) Inder J. Gupta W.D. Burnside		6. PERFORMING ORG. REPORT NUMBER ESL-711679-7
9. PERFORMING ORGANIZATION NAME AND ADDRESS The Ohio State University ElectroScience Lab Department of Electrical Engineering Columbus OH 43212		10. PROGRAM ELEMENT, PROJECT, TASK AREA & WORK UNIT NUMBERS 62702F 45196308
11. CONTROLLING OFFICE NAME AND ADDRESS Rome Air Development Center (DCCR) Griffiss AFB NY 13441		12. REPORT DATE June 1982
14. MONITORING AGENCY NAME & ADDRESS (if different from Controlling Office) Same		13. NUMBER OF PAGES 50
16. DISTRIBUTION STATEMENT (of this Report) Approved for public release; distribution unlimited		15. SECURITY CLASS. (of this report) UNCLASSIFIED
17. DISTRIBUTION STATEMENT (of the abstract entered in Block 20, if different from Report) Same		18. DECLASSIFICATION/DOWNGRADING SCHEDULE N/A
19. SUPPLEMENTARY NOTES RADC Project Engineer: Stuart H. Talbot (DCCR)		
20. KEY WORDS (Continue on reverse side if necessary and identify by block number) Adaptive Arrays Conformal Arrays Element Placement Algorithm Output Signal-to-Interference-plus-Noise Ratio (SINR) Radiation Pattern		
21. ABSTRACT (Continue on reverse side if necessary and identify by block number) An algorithm is presented which provides the appropriate element placement of an adaptive array such that the output signal-to-interference-plus-noise ratio (SINR) of the array is above a given threshold for all desired and interference signal directions. The algorithm is used to find interelement spacings of a linear as well as a conformal array. It is shown that the structure (scattered field) affects the performance of an adaptive array mounted on a complex structure such as an aircraft fuselage. A method to		

UNCLASSIFIED

SECURITY CLASSIFICATION OF THIS PAGE(When Data Entered)

take care of these effects is presented. ←

Accession For	
- TIS GRA&I <input checked="" type="checkbox"/>	
- TC TAB <input type="checkbox"/>	
- Unannounced <input type="checkbox"/>	
- Classification	
By	
Distribution/	
Availability Codes	
Dist	Avail and/or Special
A	

1000
0000
0000
0000

UNCLASSIFIED

SECURITY CLASSIFICATION OF THIS PAGE(When Data Entered)

TABLE OF CONTENTS

	Page
LIST OF FIGURES	1v
I. INTRODUCTION	1
II. FORMULATION OF THE PROBLEM	3
III. LINEAR ARRAY OF ISOTROPIC ELEMENTS	7
IV. A CONFORMAL ARRAY OF ISOTROPIC ELEMENTS	17
V. ADAPTIVE ARRAY MOUNTED ON AN AIRCRAFT	25
VI. CONCLUSION	38
REFERENCES	39

LIST OF FIGURES

Figure	Page
1. N-element adaptive array with one incident interference signal and a desired signal.	4
2. Linear array of N elements with one incident interference signal and a desired signal.	8
3. Output SINR of constraint elements versus θ_1 .	11
4. Output SINR of a three element linear array versus θ_1 .	13
5. Output SINR versus θ_1 .	14
6. Output SINR of constraint elements plus one resolution element versus θ_1 .	16
7. Output SINR of constraint elements plus two resolution elements versus θ_1 .	18
8. N-element circular array with one incident interference signal and a desired signal.	19
9. Output SINR of two axial slots (constraint elements) on a conducting cylinder versus θ_1 .	22
10. Output SINR of three axial slots (constraint elements plus one resolution element) on a conducting cylinder versus θ_1 .	24
11. Conducting cylinder with two infinite plates.	26
12. Radiation pattern of an axial slot.	27
13. Radiation pattern of an axial slot.	28

14. Output SINR of two axial slots (constraint elements versus θ_1 .)	29
15. Output SINR of three axial slots (constraint element plus one resolution element) versus θ_1 .	31
16. Radiation pattern of the resolution element.	32
17. Wing scattering effects.	33
18. Path difference between the two reflected fields.	35
19. Radiation pattern of the resolution element (—) and the compensating element (----).	36
20. Output SINR of four axial slots (constraint elements + a resolution element + a compensating element) versus θ_1 .	37

I. Introduction

It is well known that improper element patterns and/or placement can lead to dips^t in the output signal-to-interference-plus noise ratio (SINR) of an adaptive array. Ishide and Compton [1] characterized this problem in terms of a grating null phenomena and found that using elements with appropriate but unequal radiation patterns the grating nulls can be avoided. In most applications, for example an airborne adaptive array, one does not have much control on the element patterns and thus the element placement becomes important. In this paper an algorithm is presented which provides the appropriate element placement such that all the dips in the output SINR can be avoided. The algorithm is based on dividing the total number of array elements into two parts:

a) The Constraint Elements: If there are m interference signals incident on the adaptive array, at least $m+1$ elements will be needed in this part of the array. These elements are closely spaced and are placed such as to ensure that there are no dips in the output SINR. These elements will be referred to as the constraint elements and provide the required degrees of freedom.

^tWhenever the output SINR of an adaptive array drops below a certain threshold (except when the interference signal direction coincides with the desired signal direction) it will be called a dip in the output SINR. Depending upon the system requirement one can choose any threshold. In this work the input desired signal-power-to-thermal noise ratio is chosen as the threshold.

b) The Resolution Elements: Since the constraint elements are closely spaced, they may not provide the required resolution. As a result, some additional elements may be required to achieve the desired resolution. These elements are placed at large distances and constitute the resolution part of the array. These elements will be called the resolution elements.

The constraint elements are specified first. Once the spacings of the constraint elements are decided, one adds resolution elements until the required resolution is achieved without introducing extra dips.

A single incident jammer is discussed in this paper, but the method may be extended to multiple interference signals. The method is, first, applied to a linear array of isotropic elements and then it is extended to conformal arrays. It is shown that the method can be used for arrays mounted on conducting cylinders. The effect of scattered fields on the performance of an adaptive array mounted on complex structures such as an aircraft fuselage is addressed. It is shown that the scattered fields can cause extra dips in the output SINR. This specific problem is discussed in this paper and is resolved by adding additional compensating elements.

In section II an expression for the output SINR of an array of elements with identical radiation patterns in the presence of one interference signal is given. In section III this expression is used to determine the element placement of a linear array of isotropic elements. The method is extended to conformal arrays in section IV, where it is shown that the method can be used for arrays mounted on conducting

cylinders. In section V the effect of scattered fields on the performance of an adaptive array mounted on complex structures is studied. Section VI contains conclusions.

II. Formulation of the Problem

Consider an N -element adaptive array as shown in Figure 1. The elements are assumed to lie anywhere in a two dimensional space defined by the coordinates (ρ_j, θ_j) . Note that $\theta=0$ corresponds to the x -axis. Assume that two continuous wave (CW) signals at the same frequency and of same polarization are incident on the array. Let the desired and interference signals arrive from angles θ_d and θ_i , respectively. Also assume that the j th array element has a voltage response $f_j(\theta)$ with a unit amplitude signal arriving from an arbitrary angle. Then the output SINR of the array is given by [1]

$$\text{SINR} = \xi_d (U_d^T U_d^*) - \frac{|U_i^T U_d|^2}{\xi_i^{-1} + U_i^T U_i^*} \quad (1)$$

where ξ_d is the ratio of the desired signal power to the thermal noise power and ξ_i is the ratio of the interference signal power to the thermal noise power. Further, U_d is the desired signal vector which is

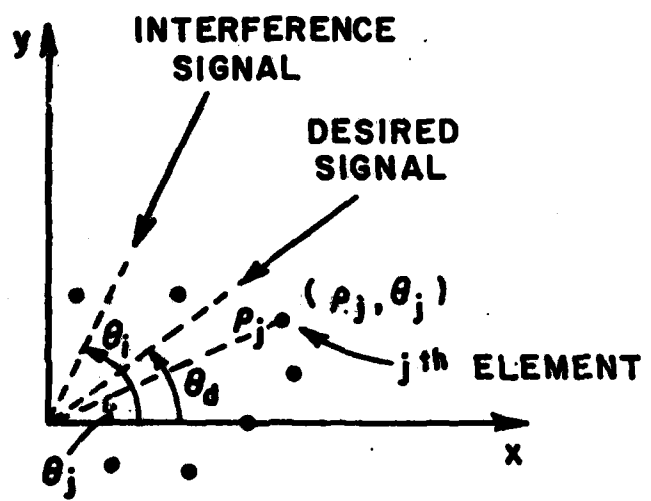


Figure 1. N -element adaptive array with one incident interference signal and a desired signal.

ned by:

$$U_d = \begin{pmatrix} f_1(\theta_d) e^{j\phi_{d1}} \\ f_2(\theta_d) e^{j\phi_{d2}} \\ \vdots \\ \vdots \\ f_N(\theta_d) e^{j\phi_{dN}} \end{pmatrix} \quad (2)$$

U_i is the interference signal vector which is defined by:

$$U_i = \begin{pmatrix} f_1(\theta_i) e^{j\phi_{i1}} \\ f_2(\theta_i) e^{j\phi_{i2}} \\ \vdots \\ \vdots \\ f_N(\theta_i) e^{j\phi_{iN}} \end{pmatrix} \quad (3)$$

In Equations (2) and (3) ϕ_{dj} and ϕ_{ij} are, respectively, the desired interference signal phase at the j^{th} element measured with respect to the coordinate origin and are given by:

$$\phi_{dj} = \frac{2\pi}{\lambda} \rho_j \cos (\theta_d - \theta_j) \quad \text{and} \quad (4)$$

$$\phi_{ij} = \frac{2\pi}{\lambda} \rho_j \cos (\theta_i - \theta_j) \quad , \quad (5)$$

where λ is the wavelength of the CW signals. For an array of elements with identical radiation patterns

$$f_1(\theta) = f_2(\theta) = \dots \dots \dots f_N(\theta) = f(\theta) , \quad (6)$$

and using (2), (3) and (6) in Equation (1) one obtains

$$\text{SINR} = \xi_d \left\{ N |f(\theta_d)|^2 - \frac{|f(\theta_1)f^*(\theta_d)|^2}{\xi_i^{-1} + N |f(\theta_1)|^2} \left| \sum_{j=1}^N e^{j(\phi_{ij} - \phi_{dj})} \right|^2 \right\} . \quad (7)$$

For strong interfering signal, i.e., $\xi_i \gg 1$ Equation (7) yields

$$\text{SINR} \approx \xi_d |f(\theta_d)|^2 \left\{ N - \frac{|f(\theta_1)f^*(\theta_d)|^2}{N \cdot |f(\theta_1)|^2 |f(\theta_d)|^2} \left| \sum_{j=1}^N e^{j(\phi_{ij} - \phi_{dj})} \right|^2 \right\} \quad (8)$$

Equation (8) will be used to find interelement spacing for the constraint elements of the adaptive array as shown later.

III. Linear Array Of Isotropic Elements

If all the elements of the array are isotropic and are placed along the x axis as shown in Figure 2, then,

$$f(\theta) = 1 \quad (9)$$

and

$$\theta_j = 0 \quad j = 1, 2, \dots, N. \quad (10)$$

Using (9) and (10) Equation (8) yields

$$\text{SINR} \approx \xi_d \left\{ N - \frac{\left| \sum_{j=1}^N \exp j(\phi_{ij} - \phi_{dj}) \right|^2}{N} \right\}, \quad (11)$$

where

$$\phi_{ij} = \frac{2\pi}{\lambda} \rho_j \cos \theta_i$$

and

$$\phi_{dj} = \frac{2\pi}{\lambda} \rho_j \cos \theta_d$$

a) Constraint element placements: In the presence of one interference signal, the constraint part of the array consists of two elements. For a two element array, Equation (11) becomes

$$\text{SINR} = \xi_d \left\{ 2 - \frac{|e^{j(\phi_{i1} - \phi_{d1})} + e^{j(\phi_{i2} - \phi_{d2})}|^2}{2} \right\}. \quad (13)$$

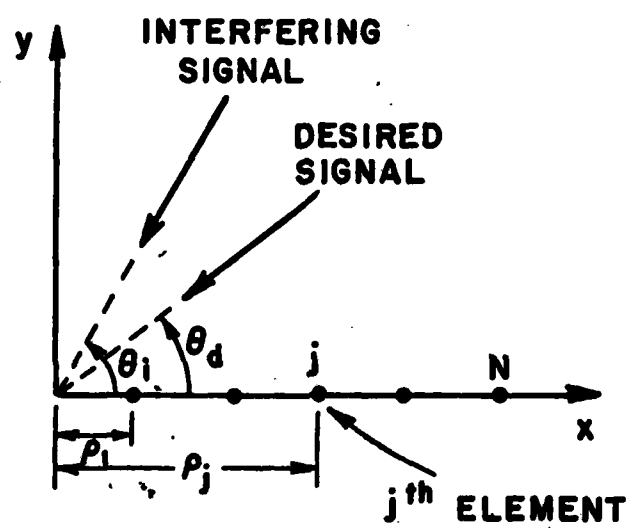


Figure 2. Linear array of N elements with one incident interference signal and a desired signal.

Using (12) in Equation (13)

$$\text{SINR} = \xi_d [1 - \cos \left\{ \frac{2\pi}{\lambda} (\rho_2 - \rho_1) (\cos \theta_f - \cos \theta_d) \right\}] . \quad (14)$$

Note that when $\theta_d = \theta_f$, the output SINR is zero[†]. Whereas, if one chooses $(\rho_2 - \rho_1)$ so that as the angular separation between the two signals increases the output SINR does not again drop below some threshold, all dips in the output SINR can be avoided. For this discussion, let us choose the threshold at ξ_d . Therefore, $(\rho_2 - \rho_1)$ should be chosen so that $\text{SINR} > \xi_d$ for all θ_d and θ_f . Using Equation (14)

$$1 > 1 - \cos \left(\frac{2\pi}{\lambda} (\rho_2 - \rho_1) (\cos \theta_f - \cos \theta_d) \right) . \quad (15)$$

The equality will be satisfied if and only if

$$\frac{2\pi}{\lambda} (\rho_2 - \rho_1) (\cos \theta_f - \cos \theta_d) = \pm \frac{2m+1}{2} \pi \quad \text{with } m=0,1,2,\dots .$$

Or,

$$\frac{\rho_2 - \rho_1}{\lambda} (\cos \theta_f - \cos \theta_d) = \pm \frac{2m+1}{4} . \quad (16)$$

Now $m=0$ in Equation (16) corresponds to the small angular separation between the two signals where the SINR will be below threshold. As $(\rho_2 - \rho_1)$ is increased, more and more values of m will satisfy Equation (16), and consequently one will obtain numerous

[†]It is assumed that $\xi_1 \gg 1$ and, consequently, the SINR will be approximately zero. Actually, $\text{SINR} \approx \xi_d / \xi_1$

dips in the output SINR. To avoid these dips m should be chosen equal to one. Then equation (16) yields

$$\left| \frac{\rho_2 - \rho_1}{\lambda} \right| < \frac{3}{4|\cos \theta_1 - \cos \theta_d|_{\max}} \quad (17)$$

Equation (17) gives the spacing between constraint elements. If one is interested in the whole visible space, i.e., $0 < \theta_d < \pi$

then

$$|\cos \theta_1 - \cos \theta_d|_{\max} = 2, \quad (18)$$

and from Equation (17)

$$\left| \frac{\rho_2 - \rho_1}{\lambda} \right| < 0.375. \quad (19)$$

Thus the constraint elements should be 0.375λ apart. Figure 3 shows the output SINR of a two element array as a function of the interference signal direction. In this plot $\theta_d=0^\circ$, $\xi_d = 1$, $\xi_1 = 100$ and the interelement spacing is 0.375λ . Note that there are no dips in the output SINR, i.e., for large angular separation between the two signals the output SINR never goes below the threshold (ξ_d in our study). On the other hand, note that the resolution of the array is very poor. In order to improve the resolution one must add some resolution elements which will complete the design.

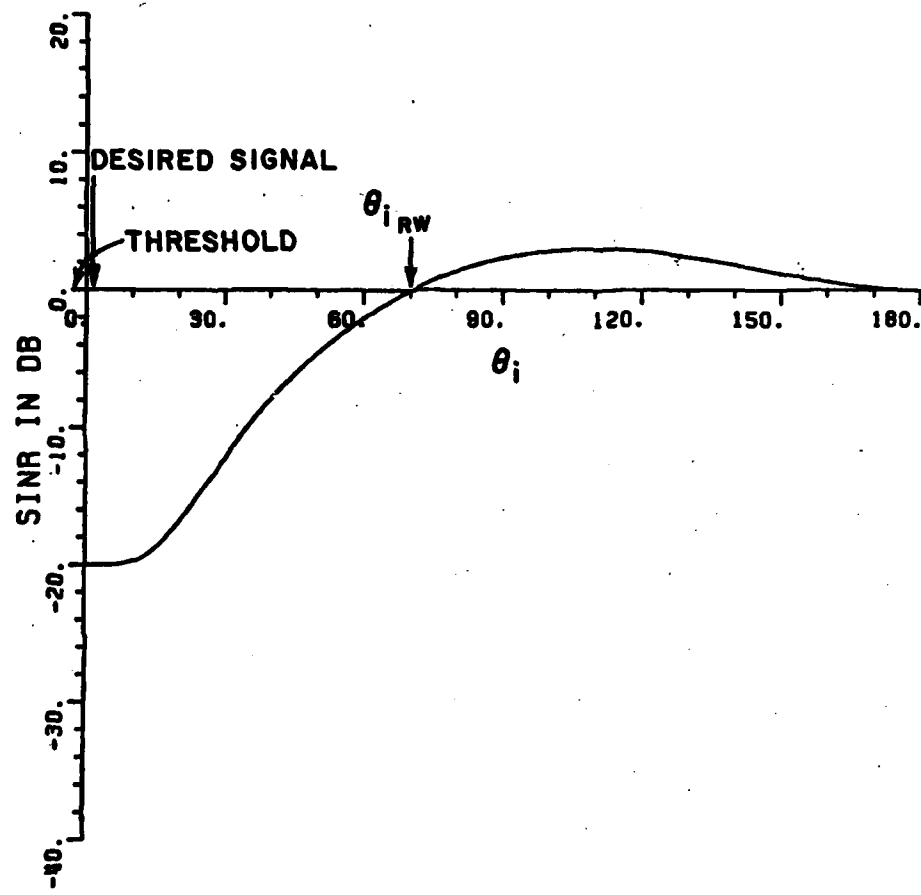


Figure 3. Output SINR of constraint elements versus θ_i .

$$\rho_1 = 0, \rho_2 = 0.375 \lambda, \theta_d = 0^\circ, \xi_d = 1, \xi_f = 100.$$

b) Resolution element placement: Since the maximum resolution of a linear adaptive array is dependent upon its total length or the distance between its end elements, one must add elements (resolution) to increase the total length of the array. If resolution elements are added to the array indiscriminately as shown in Figure 4, the output SINR of the array may, again, have dips. Note that the addition of the new element increases the resolution of the array; however as the spacing of the resolution element ($\rho_3 - \rho_1$) is increased beyond some limit a dip appears in the output SINR. This dip is undesirable and puts a limit on the spacing of the resolution element.

In order to determine the proper resolution element position, an array using only the end elements is examined. Figure 5 shows the output SINR of a three element array. The broken curve shows the output SINR due to the constraint part of the array while the continuous curve gives the output SINR due to the end elements only. One observes that the output SINR due to the end elements has grating nulls [1]. If grating nulls occur outside the resolution width[†] of the original array

[†]The minimum angular separation (between an interference signal and a desired signal) required to bring the output SINR from a null (when the two signals coincide) to the threshold will be called the resolution width (RW) of the array, and is defined as

$$RW = \frac{|\cos \theta_d - \cos \theta_{1,RW}|}{\cos \theta_{1,RW}}$$

where $\theta_{1,RW}$ is the interference angle at which the output SINR reaches the threshold. In Figure 3, $\theta_d = 0^\circ$ and $\theta_{1,RW} \approx 70^\circ$. Note that the smaller the resolution width the better is the resolution of the adaptive array.

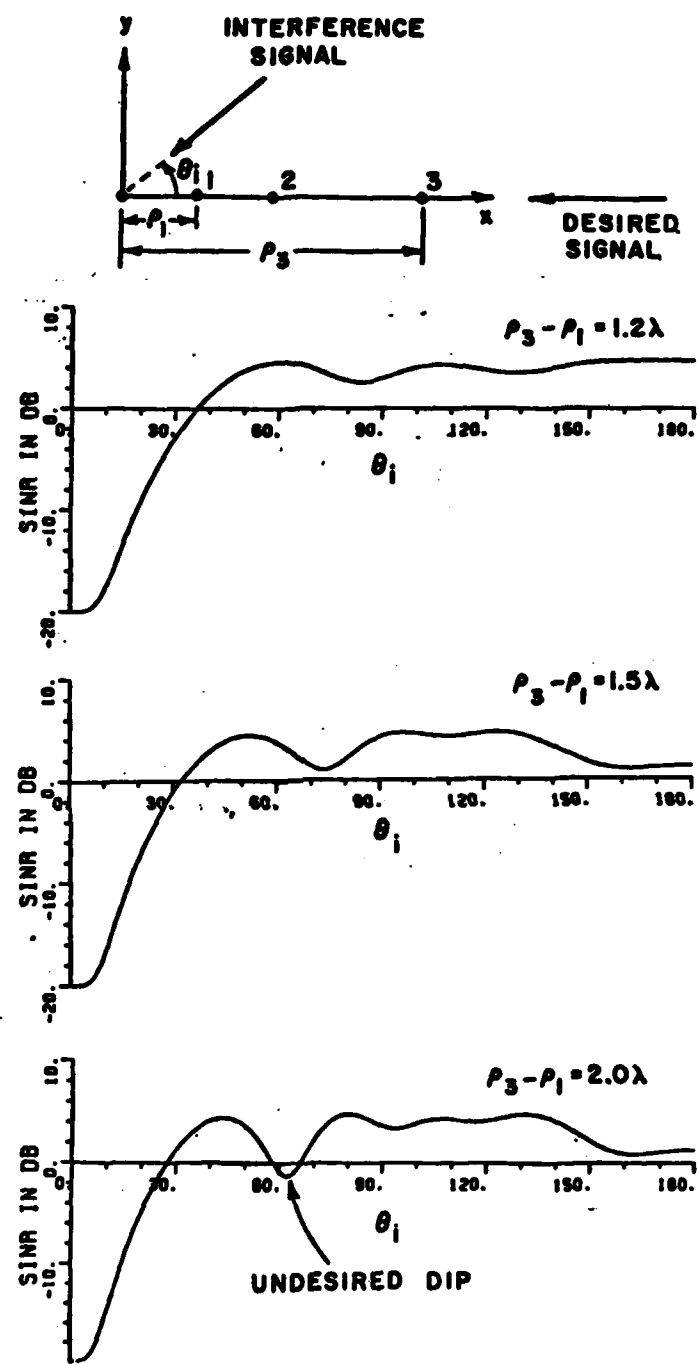


Figure 4. Output SINR of a three element linear array versus θ_i for different p_3 . $p_1 = 0$, $p_2 = 0.375\lambda$, $\theta_d = 0^\circ$, $\xi_d = 1$, $\xi_1 = 100$.

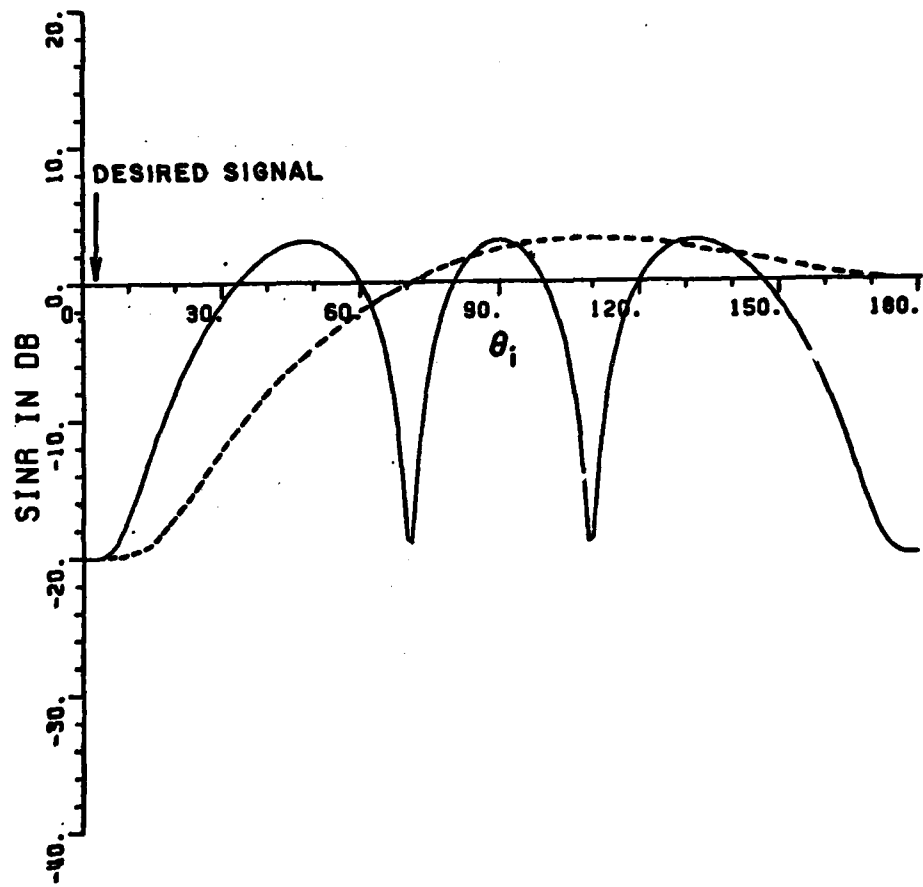


Figure 5. Output SINR versus θ_1 . (----) using constraint elements, (—) using end elements. $\rho_1 = 0.$, $\rho_2 = 0.375 \lambda$, $\rho_3 = 1.5 \lambda$, $\theta_d = 0^\circ$, $\xi_d = 1$, $\xi_1 = 100$.

(constraint part in this case) the addition of the resolution element will not cause extra dips. Consequently, in order to avoid extra dips the angular separation between the desired signal and the first grating null should be more than the resolution width of the original array. From Equation (14) the angular separation between the desired signal and the first grating null direction is

$$|\cos \theta_i - \cos \theta_d| = \frac{\lambda}{|\rho_r - \rho_1|} , \quad (20)$$

where ρ_r is the spacing of the resolution element. Therefore,

$$\frac{\lambda}{|\rho_r - \rho_1|} > RW$$

or,

$$\frac{|\rho_r - \rho_1|}{\lambda} > \frac{1}{RW} . \quad (21)$$

Thus knowing the resolution width of the original array the spacing of the next resolution element can be found. One should note that Equation (21) gives the distance between the end elements. Therefore, the resolution element can be added on either side of the original array. Now the RW using the constraint element is 0.667 (Figure 3). Hence the first resolution element should be added such that the total length of the array is less than or equal to 1.5λ (Equation (21)). Figure 6 shows the output SINR of the array containing one resolution element. It is observed that there are no dips in the output SINR and the resolution is much better than that of the original array (Figure 3).

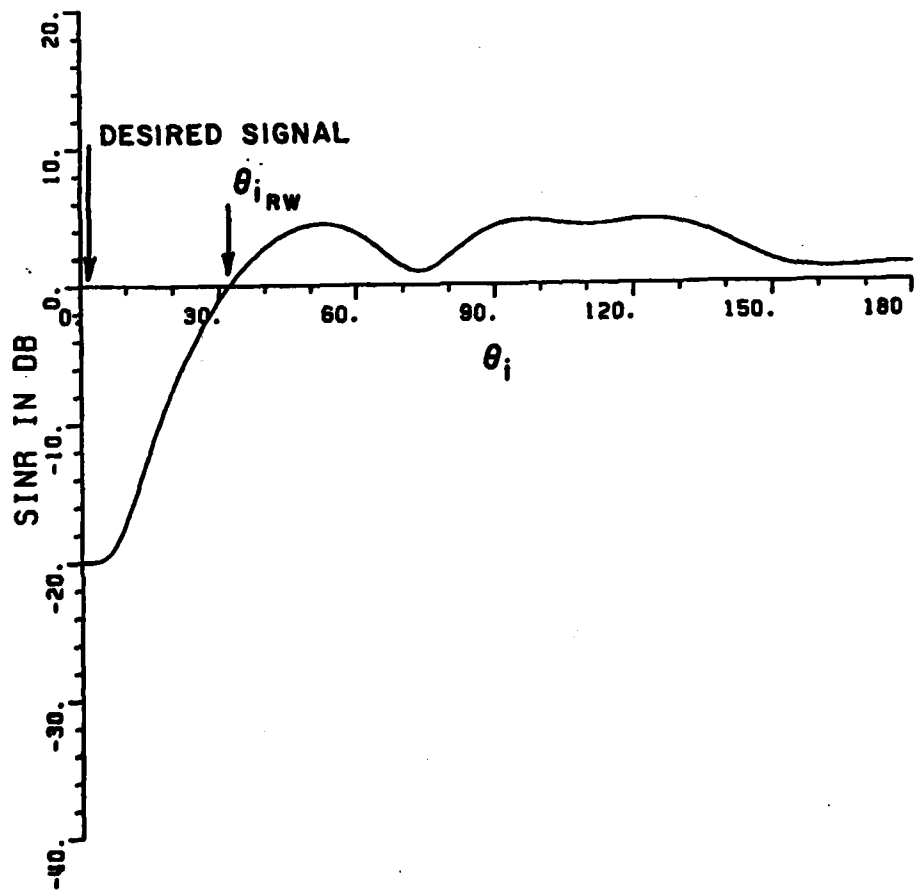


Figure 6. Output SINR of constraint elements plus one resolution element versus θ_i . $\rho_1 = 0$, $\rho_2 = 0.375\lambda$, $\rho_3 = 1.5\lambda$, $\theta_d = 0^\circ$, $\xi_d = 1$, $\xi_1 = 100$.

If one wishes to improve the resolution further, a second resolution element should be added. From Figure 6, the resolution width of the three element array is 0.15625. Using Equation (22) the total length of the new array, therefore, should be $< 6.4 \lambda$. Figure 7 shows the output SINR of the array containing two prescribed resolution elements. Again there are no dips in the output SINR and the resolution has greatly improved. Thus one can achieve as much resolution as one wishes provided that the number of elements and the array size does not exceed other requirements.

IV. A Conformal Array of Isotropic Elements

If all the elements of the array are isotropic and are placed along a circle of radius r as shown in Figure 8, then Equation (8) becomes

$$\text{SINR} \approx E_d \left\{ N - \frac{\left| \sum_{j=1}^N \exp(\phi_{ij} - \phi_{dj}) \right|^2}{N} \right\} , \quad (22)$$

where

$$\begin{aligned} \phi_{ij} &= \frac{2\pi}{\lambda} r \cos(\theta_i - \theta_j) \\ \phi_{dj} &= \frac{2\pi}{\lambda} r \cos(\theta_d - \theta_j) \end{aligned} \quad (23)$$

a) Constraint element placement: In the presence of one interference signal the constraint part of the array consists of two

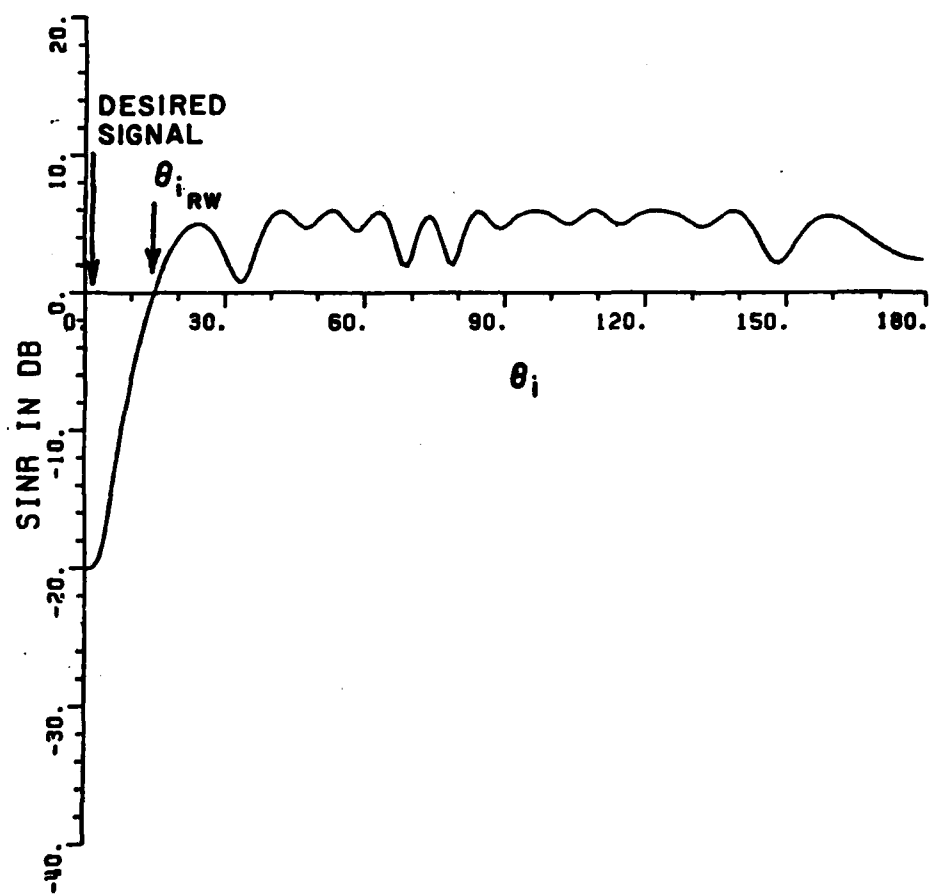


Figure 7. Output SINR of constraint elements plus two resolution elements versus θ_i . $\rho_1=0$, $\rho_2=0.375\lambda$, $\rho_3=1.5\lambda$, $\rho_4=6.4\lambda$, $\theta_d=0^\circ$, $\xi_d=1$, $\xi_1=100$.

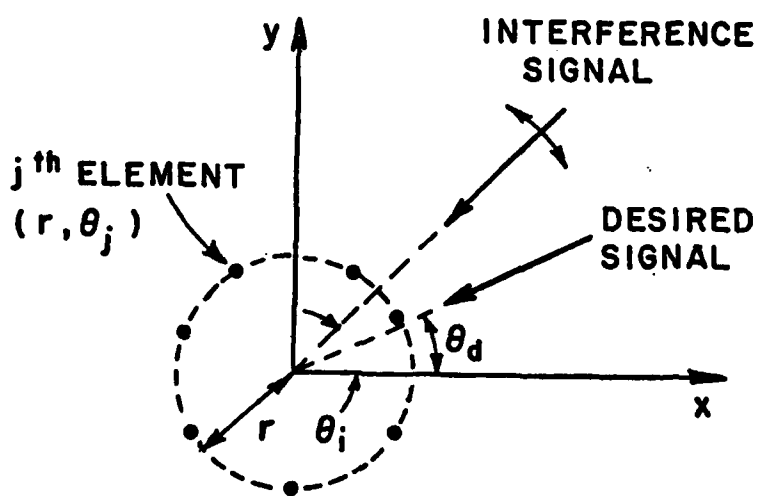


Figure 8. N -element circular array with one incident interference signal and a desired signal.

elements. Let these elements be placed symmetrically about the y-axis, i.e.,

$$\theta_2 = \pi - \theta_1 \quad (24)$$

then Equation (22) yields

$$\text{SINR} \approx \xi_d \left(1 - \cos \frac{(2\pi r g)}{\lambda} \right) \quad (25)$$

where

$$g = \cos(\theta_i - \theta_2) - \cos(\theta_d - \theta_2) - \cos(\theta_i - \theta_1) + \cos(\theta_d - \theta_1) \quad (26)$$

Using (24), Equation (26) yields

$$g = 2 \cos \theta_1 \cdot (\cos \theta_d - \cos \theta_i) \quad (27)$$

Substituting (27) in Equation (26), one obtains

$$\text{SINR} \approx \xi_d \left\{ 1 - \cos \left(\frac{4\pi r}{\lambda} \cos \theta_1 \cdot (\cos \theta_d - \cos \theta_i) \right) \right\} \quad (28)$$

Then using the same arguments as done earlier, one can find θ_1 so that there are no dips in the output SINR. Following the same procedure one obtains

$$\theta_1 = \cos^{-1} \left(\frac{3\lambda}{8r|\cos \theta_d - \cos \theta_i|_{\max}} \right) \quad (29)$$

If $\frac{\pi}{9} < \theta_d < \frac{8\pi}{9}$, i.e., the field of view is $(20^\circ, 160^\circ)$ and $r = 3.2\lambda$, Equation (30) yields $\theta_1 = 86.425^\circ$.

If instead of free space, the array elements are placed on the surface of an infinite conducting cylinder, the radiation patterns of

the constraint elements will be similar. Further, for $\frac{\pi}{9} < \theta_d < \frac{8\pi}{9}$ Equation (8) can be approximated as

$$\text{SINR} = \xi_d |f(\theta_d)|^2 \left\{ N - \frac{\left| \sum_{j=1}^N \exp(\phi_{ij} - \phi_{dj}) \right|^2}{N} \right\} \quad (30)$$

where ϕ_{ij} and ϕ_{dj} are given in Equation (23). Note that (30) differs from (22) in that the first one is multiplied by a factor $|f(\theta_d)|^2$. As the array elements are placed on a conducting cylinder $|f(\theta_d)| > 1$, hence one can use a larger spacing between the constraint elements.

Figure 9 shows the output SINR of a two element (axial slot) array on an infinite conducting cylinder of radius 3.2λ . The elements are placed at $\theta_1=94^\circ$ and $\theta_2=86^\circ$, respectively. Again it is observed that there are no dips in the output SINR. The resolution width of the array (RW) is 0.380, which is quite poor. In order to increase the resolution one needs to add some resolution elements.

b) Resolution element placement: From Equation (25) one observes that the output SINR will have a grating null whenever:

$$\frac{2\pi r}{\lambda} g = \pm 2 m \pi \quad (31)$$

$m = 1, 2, \dots$, or

$$g = \pm \frac{m\lambda}{r} . \quad (32)$$

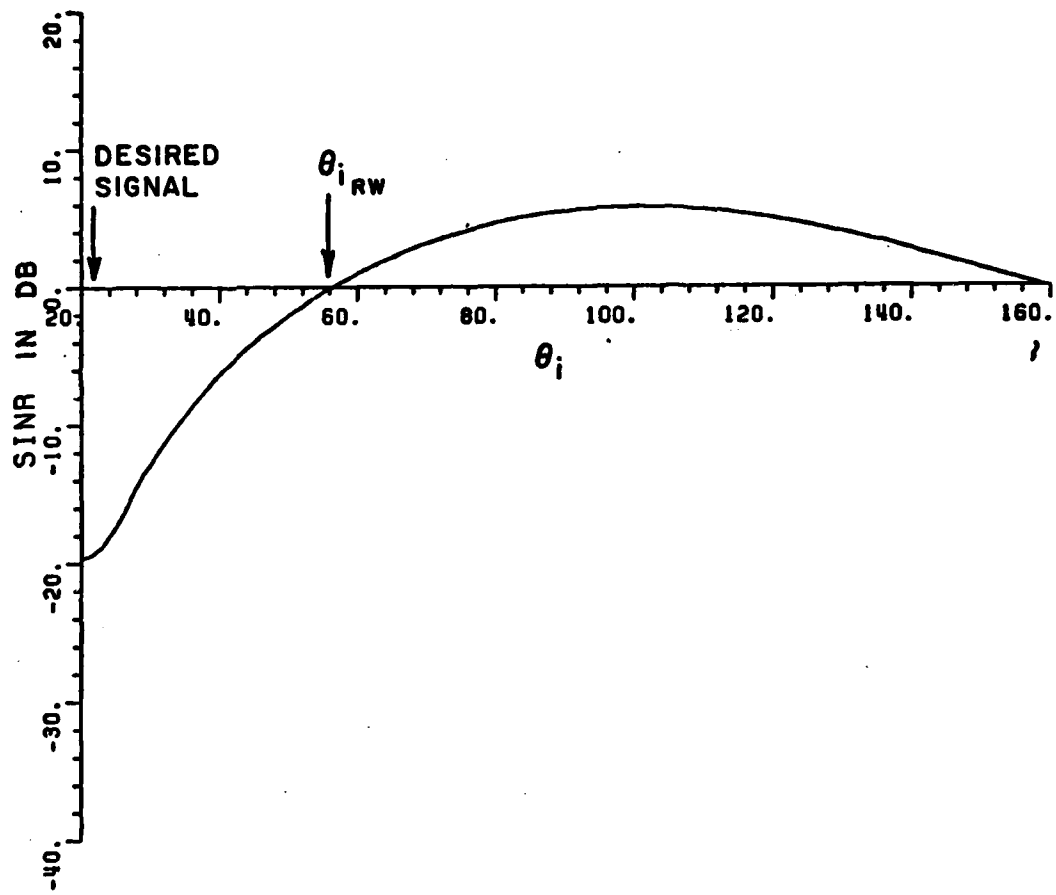


Figure 9. Output SINR of two axial slots (constraint elements) on a conducting cylinder versus θ_i . $\theta_1=94^\circ$, $\theta_2=86^\circ$, $\theta_d=20^\circ$, $\xi_d=1$, $\xi_f=100$, $r=3.2\lambda$.

Using (26)

$$\cos(\theta_i - \theta_2) - \cos(\theta_d - \theta_2) - \cos(\theta_i - \theta_1) + \cos(\theta_d - \theta_1) = \pm \frac{m\lambda}{r} . \quad (33)$$

In order to avoid dips in the output SINR, the first grating null must fall outside the resolution width of the old array. Therefore,

$$\begin{aligned} \cos(\theta_{i_{RW}} - \theta_r) - \cos(\theta_d - \theta_r) - \\ \cos(\theta_{i_{RW}} - \theta_1) + \cos(\theta_d - \theta_1) = \pm \frac{\lambda}{r} \end{aligned} \quad (34)$$

where θ_r defines the location of the resolution element and $\theta_{i_{RW}}$ defines the resolution width of the old array. Since $\theta_{i_{RW}}$, θ_d and θ_1 are known, one can solve for θ_r using Equation (34).

For the array in Figure 9, $\theta_1=94^\circ$, $\theta_d=20^\circ$ and $\theta_{i_{RW}}=56^\circ$. Solving Equation (34) for these values one obtains $\theta_r \approx 56.0^\circ$. Figure 10 shows the output SINR of a three element (axial slot) array on an infinite conducting cylinder of radius 3.2λ . The elements are placed at $\theta_1=94^\circ$, $\theta_2=86^\circ$ and $\theta_3=56.0^\circ$. The array provides the desired resolution without introducing additional dips in the output SINR. This completes the design procedure as it applies to simple structures. An important aspect of this procedure remains to be answered in terms of its real life adequacy. What if the resolution element does not have enough radiation for $\theta > 90^\circ$? In such a case the array will have poor resolution for $\theta_d > 90^\circ$. This problem can be easily resolved by building a symmetrical array, i.e., by adding another resolution element at $\theta=124^\circ$.

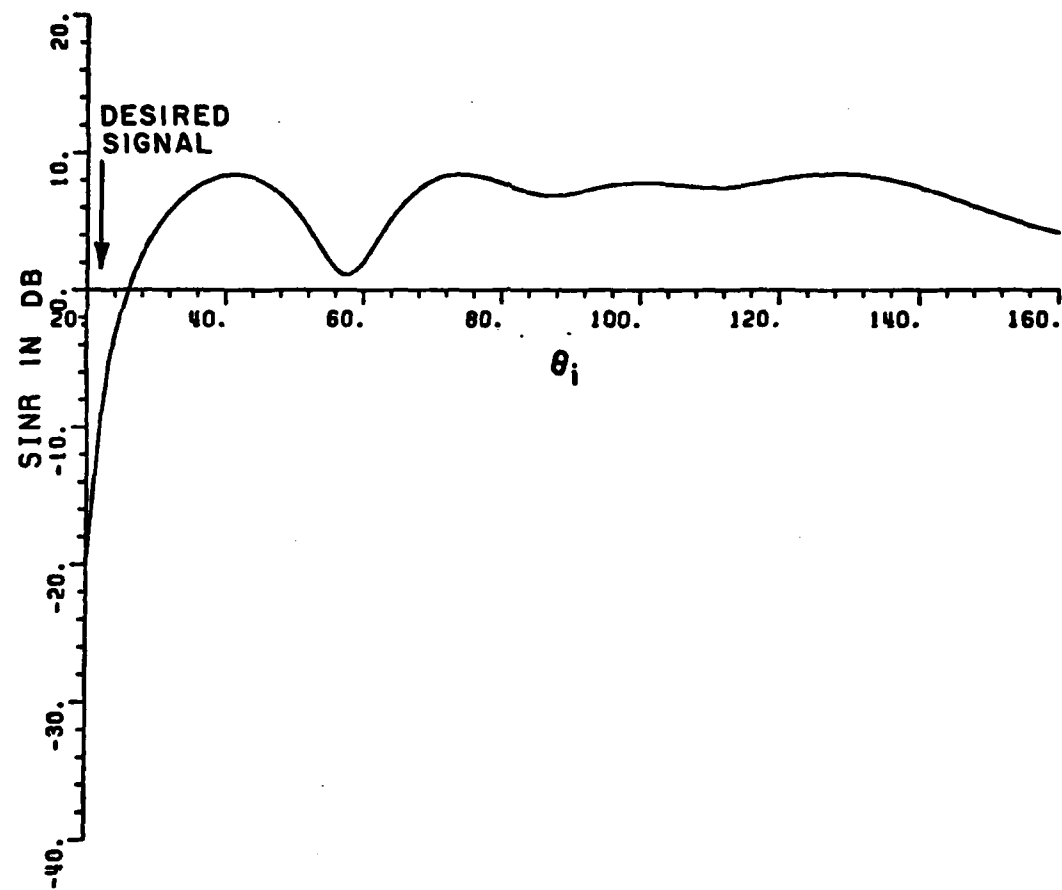


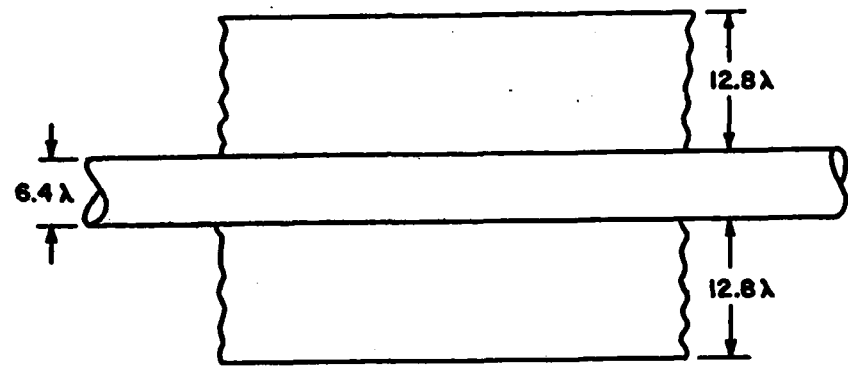
Figure 10. Output SINR of three axial slots (constraint elements plus one resolution element) on a conducting cylinder versus θ_i . $\theta_1=94^\circ$, $\theta_2=86^\circ$, $\theta_3=56^\circ$, $\theta_d=20^\circ$, $\xi_d=1$, $\xi_1=100$, $r=3.2\lambda$.

V. Adaptive Array Mounted On An Aircraft

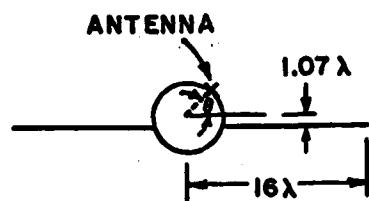
For an antenna mounted on an aircraft there is a scattered field from the wings, stabilizers, nose, etc. The scattered field affects the radiation pattern of the antenna and sometimes causes deep nulls in the radiation pattern. Let us consider an infinite conducting cylinder of radius 3.2λ to which are attached two conducting plates as shown in Figure 11. Figure 12 shows the radiation pattern of an axial slot with and without plates. The slot is mounted on the top of cylinder at $\theta=90^\circ$. Note that the scattered fields from plates have changed the radiation characteristic of the slot, but there are no deep nulls in the radiation pattern.

Figure 13 shows the radiation pattern of the axial slot when the slot is moved towards the right plate. In this case, there are deep nulls in the radiation pattern and the radiation is weak on the other side of the structure ($90^\circ < \theta < 180^\circ$). Thus the scattered field becomes more significant as the antenna moves closer to the plates. In most applications an adaptive array is required to provide omnidirectional coverage around an aircraft. The constraint elements, therefore, should be mounted along or near the aircraft center line. The resolution elements on the other hand are widely spaced and most likely positioned at wide angles around the fuselage. As a result, the resolution element pattern will be more affected by the wings than the constraint elements. This distortion effect is examined next in terms of the output SINR of an adaptive array.

Figure 14 shows the output SINR due to the constraint part of an adaptive array mounted on the structure shown in Figure 11. The



(a) TOP VIEW



(b) FRONT VIEW

Figure 11. Conducting cylinder with two infinite plates.

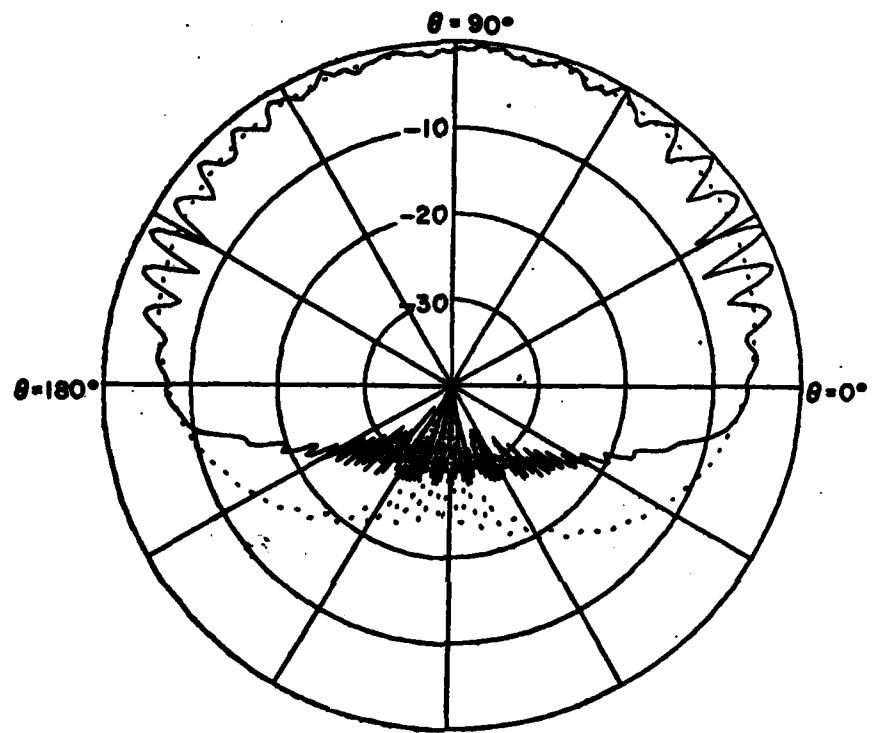


Figure 12. Radiation pattern of an axial slot mounted on a circular cylinder ($\theta_3 = 90^\circ$). (—) with plates and (----) without plates.

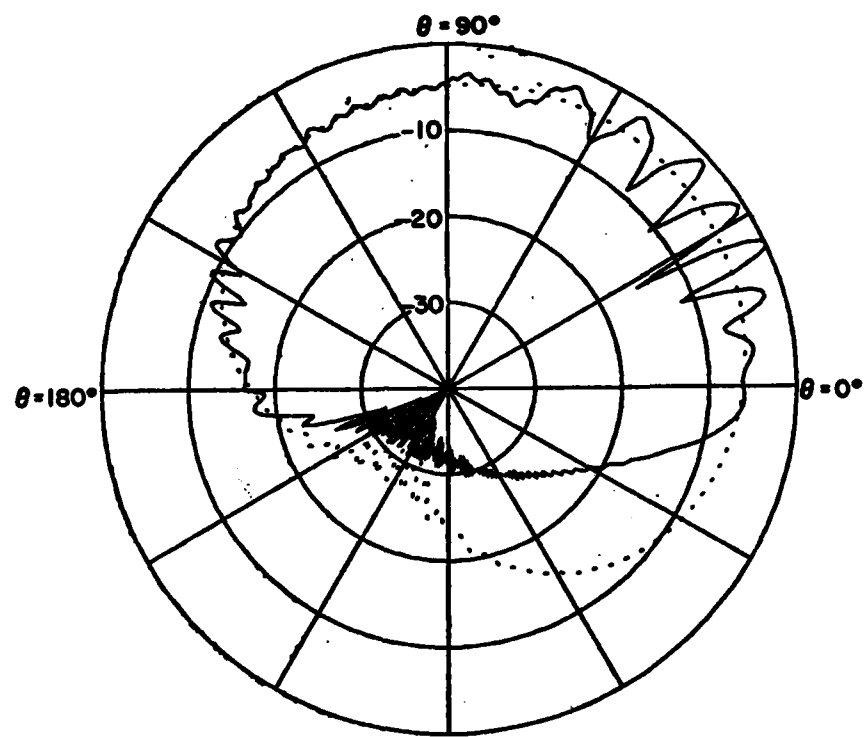


Figure 13. Radiation pattern of an axial slot mounted on the side ($\theta_s=56^\circ$) of a circular cylinder. (—) with plates and (----) without plates.

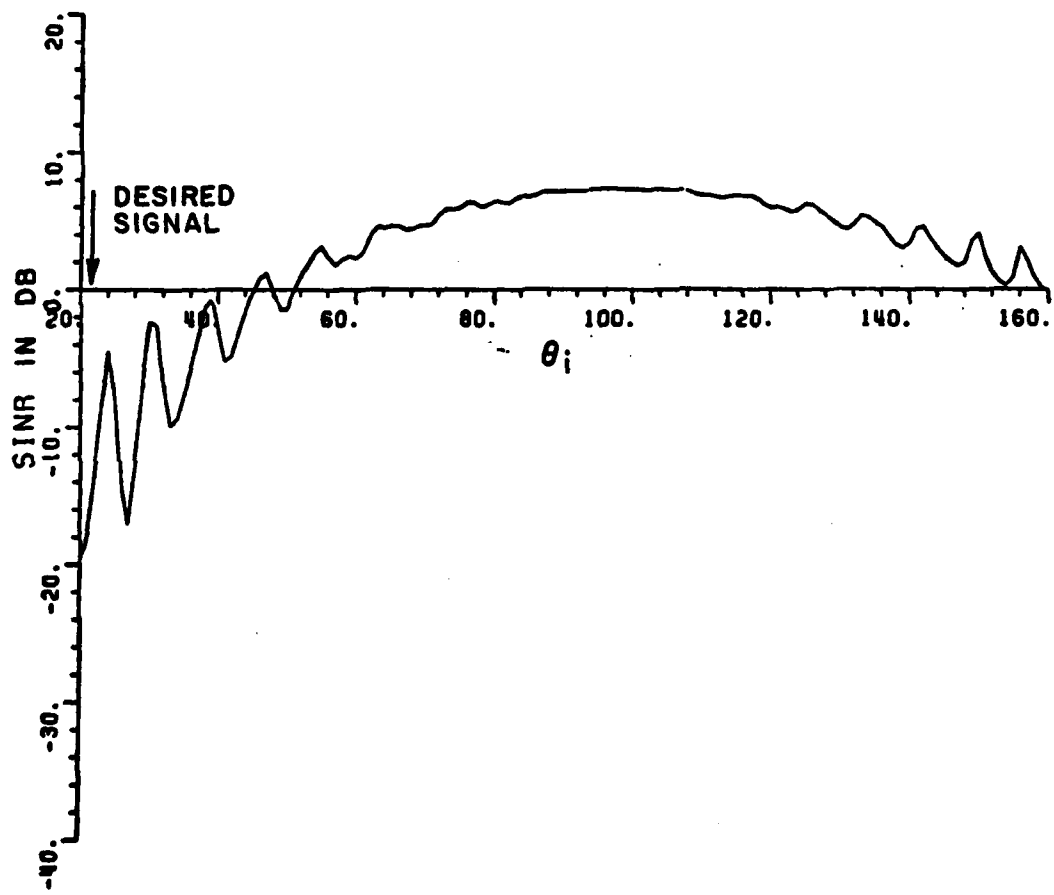


Figure 14. Output SINR of two axial slots (constraint elements)
versus θ_i . $\theta_1=94^\circ$ $\theta_2=86^\circ$, $\theta_d=20^\circ$, $\xi_d=1$, $\xi_f=100$

constraint elements are placed at $\theta_1=94^\circ$ and $\theta_2=86^\circ$, respectively. It is observed that the output SINR due to the constraint part is the same as of the array mounted on a circular cylinder without any plates (Figure 9). The small oscillations in the output SINR are due to the oscillations in the radiation pattern of the individual elements. Further, there are no significant dips in the output SINR, but the resolution of the array is quite poor ($RW \sim 0.380$). In order to improve the resolution, a resolution element should be added to the array. In section IV, it was shown that the resolution element should be placed at $\theta_5=56.0^\circ$. Figure 15 shows the output SINR of the array with one prescribed resolution element. Note that the resolution of the array has improved; however, there is a dip in the output SINR. In order to avoid this dip one may need an extra element which shall be called a "compensating element".

Before discussing the placement of the compensating element, one needs to understand the reason for the dip in the output SINR. Figure 16 shows the radiation pattern of the resolution element. Note that the radiation pattern has a deep null at $\theta \sim 28^\circ$. This null appears as a dip in the output SINR. The reason for a deep null in the radiation pattern is the strong reflected field from the plates as shown in Figure 17 (a). This reflected field interferes destructively and constructively with the direct field to cause nulls and peaks in the radiation pattern. The null directions depend on the location of antenna and its image in the plate. If one adds another antenna element so that the reflected fields of two antennas are out of phase (see Figure 17 (b)), then one antenna

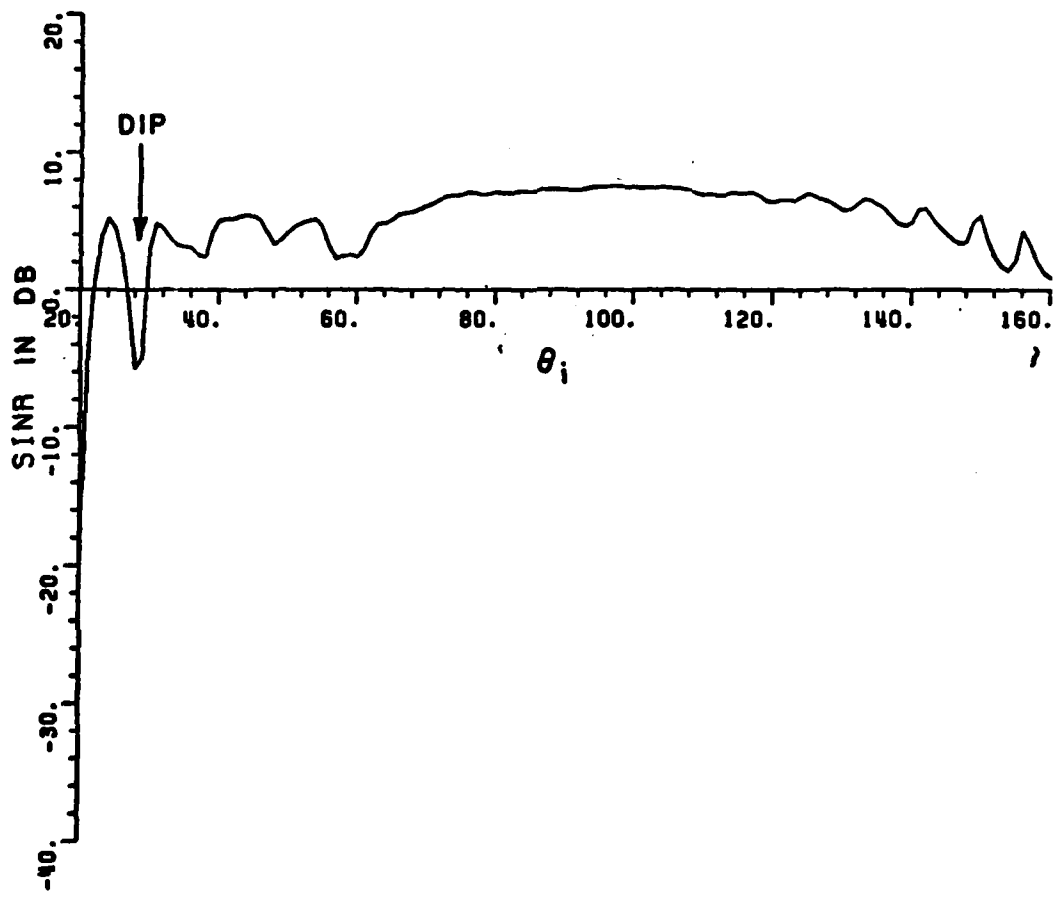


Figure 15. Output SINR of three axial slots (constraint element plus one resolution element) versus θ_i . $\theta_1=94^\circ$, $\theta_2=86^\circ$, $\theta_3=56^\circ$, $\theta_d=20^\circ$, $\xi_d=1$, $\xi_f=100$.

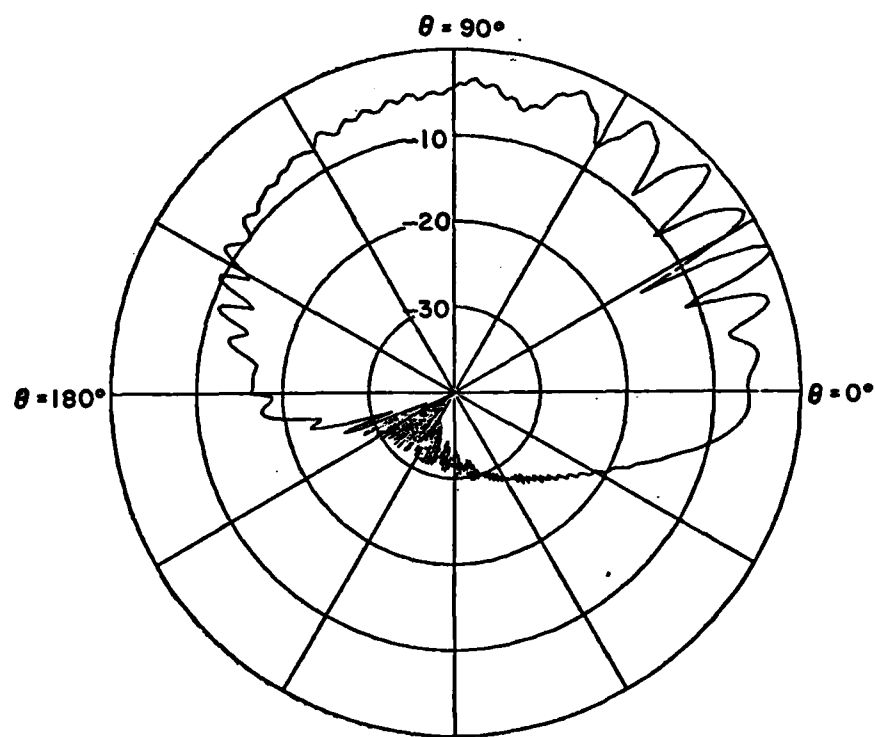
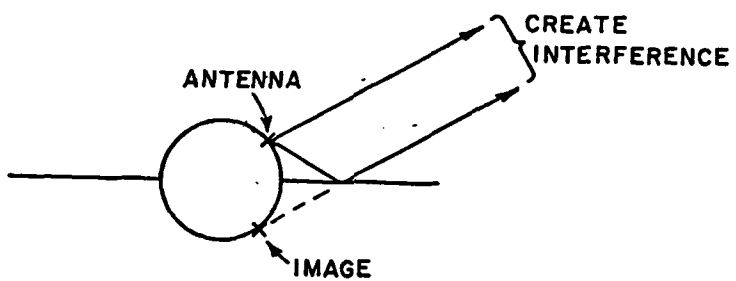
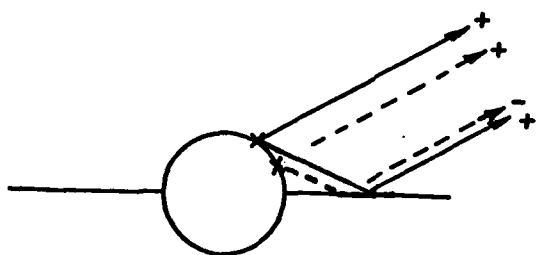


Figure 16. Radiation pattern of the resolution element.



(a) EFFECT OF WING SCATTERING



(b) TWO REFLECTED FIELDS ARE OUT OF PHASE

Figure 17. Wing Scattering Effects.

will have a peak while the other has a null in the same direction. The second antenna then can be used as a compensating element. One can find the approximate location of the compensating element as follows.

From Figure 18 the two reflected fields will be out of phase, if

$$\frac{2\pi}{\lambda} (A' C' - B' D') = \pi \quad (35)$$

Or, $\frac{2}{\lambda} (2 (r \sin \theta_A + \Delta) \cos \theta - 2 (r \sin \theta_B + \Delta) \cos \theta) = 1$

$$4 \frac{r}{\lambda} \cos \theta (\sin \theta_A - \sin \theta_B) = 1 \quad (36)$$

Knowing r , θ_A and θ one can solve for θ_B . For the structure shown in Figure 11, $r=3.2\lambda$ and the resolution element is placed at $\theta_3=\theta_A = 56^\circ$. The dip occurs at $\theta \approx 28^\circ$. Hence, using Equation (36) the compensating element should be placed at $\theta_B = 47.75^\circ$.

Figure 19 shows the radiation patterns of the resolution element (axial slot at $\theta=56^\circ$) and the compensating element (axial slot at $\theta=47^\circ$). Note that this arrangement of two elements provides the necessary pattern coverage from at least one of the two resolution elements. Figure 20 shows the output SINR of a four element adaptive array mounted on the structure shown in Figure 11. The four axial slots are located at $\theta_1 = 94^\circ$, $\theta_2 = 85^\circ$, $\theta_3 = 56^\circ$ and $\theta_4 = 47^\circ$. Note that there are no dips in the output SINR and the array has good resolution. Thus, the previously described design procedure can be used to find the various array element locations for adaptive arrays mounted on complicated structures. The different steps in the algorithm are:

- a) Find the interelement spacings for the constraint elements.

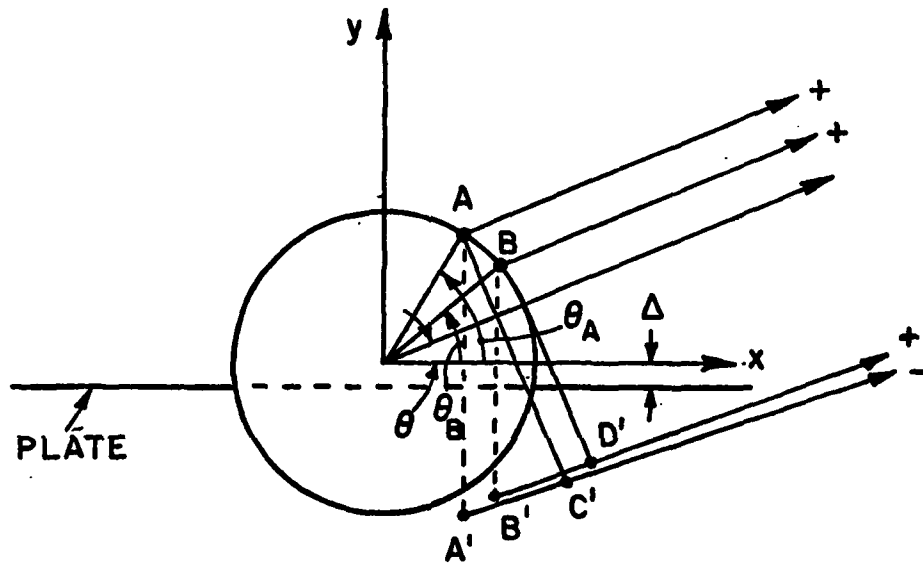


Figure 18. Path difference between the two reflected fields.

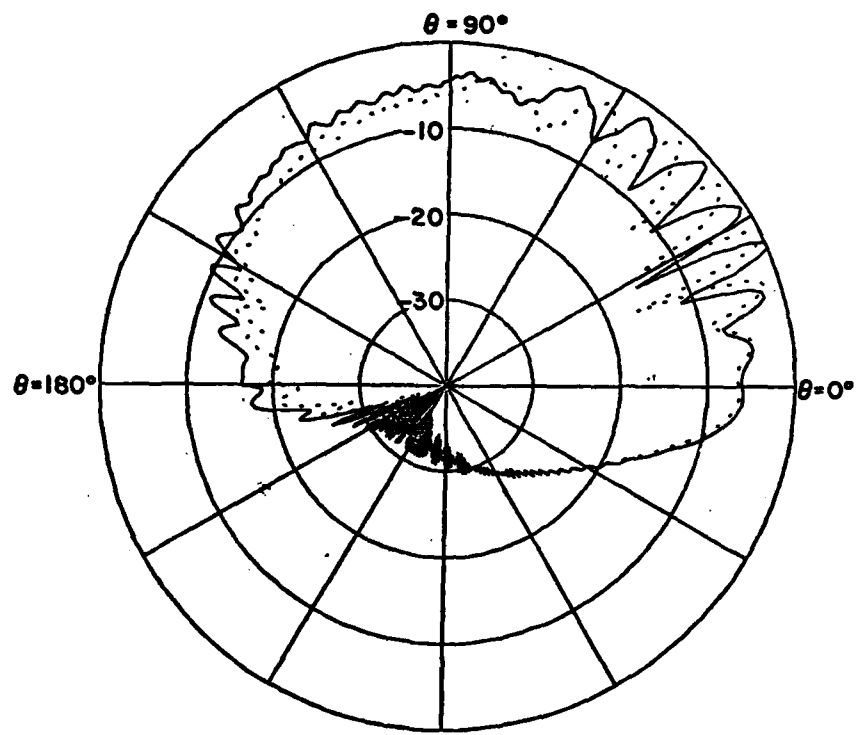


Figure 19. Radiation pattern of the resolution element (—) and the compensating element (----).

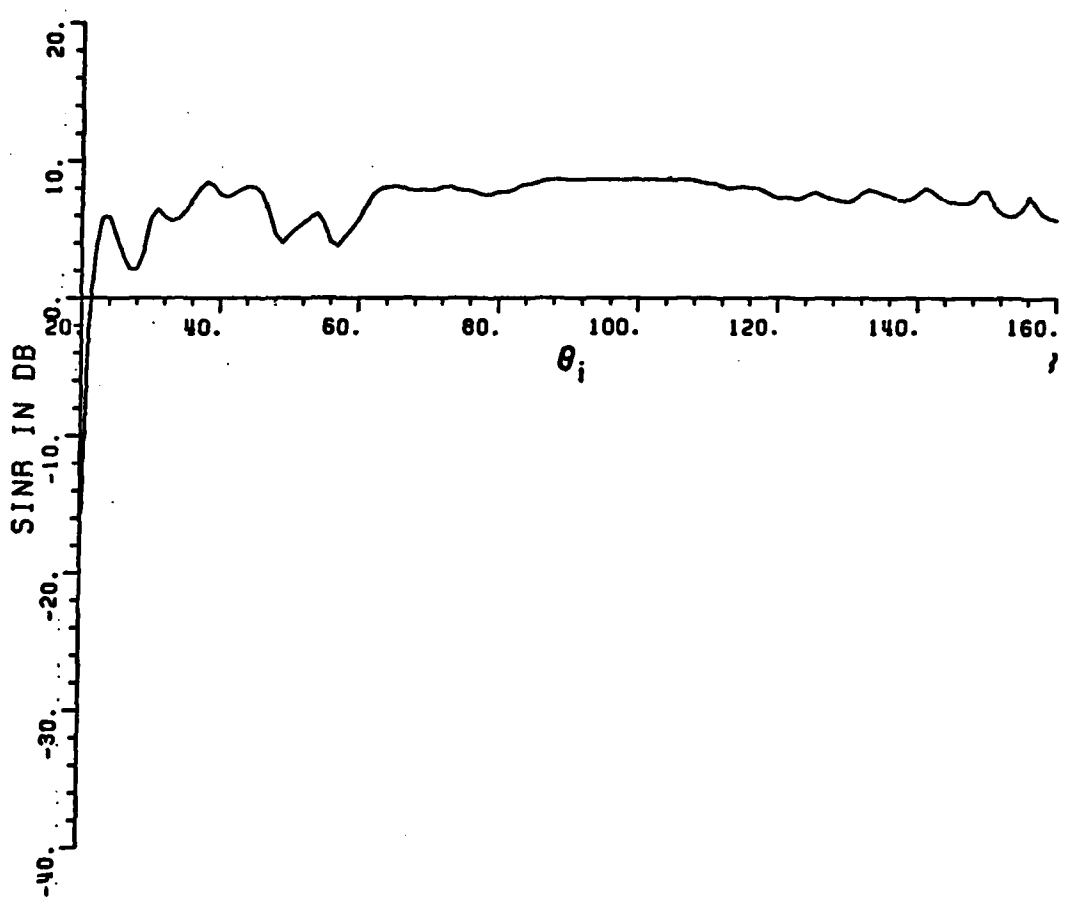


Figure 20. Output SINR of four axial slots (constraint elements + a resolution element + a compensating element) versus θ_i . $\theta_1 = 94^\circ$, $\theta_2 = 86^\circ$, $\theta_3 = 56^\circ$, $\theta_4 = 47^\circ$, $\theta_d = 20^\circ$, $\xi_d = 1$, $\xi_i = 100$.

- b) Add a resolution element to improve the resolution of the array without introducing extra dips.
- c) The resolution element should have uniform coverage in the given sector of interest. If the resolution element has nulls in its radiation pattern, add compensating element to provide necessary pattern coverage.
- d) Repeat steps (b) and (c) till the desired resolution is achieved.

VI. Conclusion

The purpose of this paper was to present an algorithm which provides the appropriate element placement of an adaptive array such that the output SINR of the array is above a given threshold for all desired and interference signal directions. Such an algorithm is developed and it is shown that the algorithm can be used to find the array element locations for adaptive arrays mounted on complicated structures. The most important conclusion to be drawn is that for good performance the adaptive array elements should have approximately uniform coverage in the desired sector of interest.

REFERENCES

1. A. Ishide and R.T. Compton, Jr., "On Grating Nulls in Adaptive Arrays," IEEE Trans. on Antennas and Propagation, Vol. AP-28, pp. 467-475, July 1980.

